NAVAL
POSTGRADUATE
SCHOOL

MONTEREY, CALIFORNIA

THESIS

RADIATION DOSE ANALYSIS OF NPS FLASH X-RAY FACILITY USING SILICON PIN DIODES

by

Bernard L. Jones

September 2003

Thesis Advisor:	Todd R. Weatherford
Second Reader:	Andrew A. Parker

Approved for public release; distribution is unlimited

THIS PAGE INTENTIONALLY LEFT BLANK

REPORT DOCUMENTATION PAGE			Form Approved OMB No. 0704-0188
Public reporting burden for this collection of information is estimated to average 1 hour per response, including the time for reviewing instruction, searching existing data sources, gathering and maintaining the data needed, and completing and reviewing the collection of information. Send comments regarding this burden estimate or any other aspect of this collection of information, including suggestions for reducing this burden, to Washington Headquarters Services, Directorate for Information Operations and Reports, 1215 Jefferson Davis Highway, Suite 1204, Arlington, VA 22202-4302, and to the Office of Management and Budget, Paperwork Reduction Project (0704-0188) Washington DC 20503.			
1. AGENCY USE ONLY *(Leave blank)*	**2. REPORT DATE** September 2003	**3. REPORT TYPE AND DATES COVERED** Master's Thesis	
4. TITLE AND SUBTITLE: Radiation dose analysis of NPS Flash X-ray facility using silicon PIN diode			**5. FUNDING NUMBERS**
6. AUTHOR(S) Bernard L. Jones			
7. PERFORMING ORGANIZATION NAME(S) AND ADDRESS(ES) Naval Postgraduate School Monterey, CA 93943-5000			**8. PERFORMING ORGANIZATION REPORT NUMBER**
9. SPONSORING /MONITORING AGENCY NAME(S) AND ADDRESS(ES) N/A			**10. SPONSORING/MONITORING AGENCY REPORT NUMBER**
11. SUPPLEMENTARY NOTES The views expressed in this thesis are those of the author and do not reflect the official policy or position of the Department of Defense or the U.S. Government.			
12a. DISTRIBUTION / AVAILABILITY STATEMENT Approved for public release; distribution is unlimited			**12b. DISTRIBUTION CODE**

13. ABSTRACT ***(maximum 200 words)***

Radiation output of the NPS Flash X-ray facility has been analyzed using commercial silicon PIN diodes. These results have been compared to dosimetry techniques using CaF_2 TLDs (thermoluminescent dosimeters). The silicon PIN diodes were irradiated with photon energies of approximately 1 MeV and dose rates up to 10^{10} rad(Si)/s. These techniques and results can be used to provide real time calibration of the Flash X-ray facility.

14. SUBJECT TERMS silicon radiation detectors, flash x-ray, dosimetry, thermoluminescent dosimeters			**15. NUMBER OF PAGES** 59
			16. PRICE CODE
17. SECURITY CLASSIFICATION OF REPORT Unclassified	**18. SECURITY CLASSIFICATION OF THIS PAGE** Unclassified	**19. SECURITY CLASSIFICATION OF ABSTRACT** Unclassified	**20. LIMITATION OF ABSTRACT** UL

NSN 7540-01-280-5500 Standard Form 298 (Rev. 2-89)
Prescribed by ANSI Std. 239-18

THIS PAGE INTENTIONALLY LEFT BLANK

Approved for public release; distribution is unlimited

RADIATION DOSE ANAYLSIS OF NPS FLASH X-RAY FACILITY USING SILICON PIN DIODE

Bernard L. Jones
Lieutenant, United States Navy
B.S., Clark Atlanta University, 1996

Submitted in partial fulfillment of the
requirements for the degree of

MASTER OF SCIENCE IN ELECTRICAL ENGINEERING

from the

NAVAL POSTGRADUATE SCHOOL
September 2003

Author: Bernard Jones

Approved by: Todd R. Weatherford
Thesis Advisor

Andrew A. Parker
Second Reader

John P. Powers
Chairman, Department of Electrical and Computer Engineering

THIS PAGE INTENTIONALLY LEFT BLANK

ABSTRACT

Radiation output of the NPS Flash X-ray facility has been analyzed using commercial silicon PIN diodes. These results have been compared to dosimetry techniques using CaF_2 TLDs (thermoluminescent dosimeters). The silicon PIN diodes were irradiated up with photon energies of approximately 1 MeV and dose rates up to 10^{10} rad(Si)/s. These techniques and results can be used to provide real time calibration of the Flash X-ray facility.

THIS PAGE INTENTIONALLY LEFT BLANK

TABLE OF CONTENTS

THIS PAGE INTENTIONALLY LEFT BLANK

LIST OF FIGURES

THIS PAGE INTENTIONALLY LEFT BLANK

LIST OF TABLES

THIS PAGE INTENTIONALLY LEFT BLANK

ACKNOWLEDGMENTS

I would like to thank Professor Todd Weatherford and Andrew Parker for their time and support. In addition, I would like to thank Mr. Don Snyder for his assistance at the Flash X-ray facility and Mr. John Retzler and Sam Rainwater for their technical insight in conducting this research.

Finally, I would like to thank my parents, family and friends for their encouragement and my wife, Tamice, for her love and support.

THIS PAGE INTENTIONALLY LEFT BLANK

EXECUTIVE SUMMARY

The Naval Postgraduate School Center for Radiation Hardened Electronics conducts research in the area of electronics for Department of Defense space and strategic systems. The NPS Flash X-ray facility provides a source of radiation for experimentation in this field of study. Installed in 1988, the Flash X-ray facility uses thermoluminescent dosimeters (TLDs) as the preferred method of radiation detection for experimentation dose levels. Semiconductor devices have been practically employed as radiation detectors since the early 1960s and technology in this field of study have vastly improved since then. This thesis is part of the effort to seek alternate means of dosimetry for the Flash X-ray facility. PIN diode dosimetry will provide real time measurements that will increase efficiency in performing experiments at the Flash X-ray facility.

Silicon photodiodes are semiconductor devices that are responsive to high energy particles and photons. Silicon photodiodes operate by the absorption of an incident particle or photon that creates an electron–hole pair through ionization. The required energy to produce an electron–hole pair is 3.6 eV. This freed pair, under the influence of an applied electric field, generates current in the device. The amplitude of the current signal is directly proportional to the free charge created within the detector. The goal of this thesis is to correlate the output signal of silicon PIN diodes to the absorbed dose of thermoluminescent dosimeters. One issue which was examined was whether measuring the waveform amplitude peak or the waveform integral would provide more precise correlation to the TLD readings. The calculated results using voltage amplitude peak provide a closer correlation more accurately to TLD readings than waveform integral results.

THIS PAGE INTENTIONALLY LEFT BLANK

I. INTRODUCTION

A. PURPOSE

Semiconductor devices are an excellent choice for radiation detection applications. Semiconductor detectors provide good energy resolution of converting incident radiant energy to an electrical signal. Current practice for dosimetry at the NPS Flash X-ray facility is thermoluminescent dosimeters (TLDs). Even though the use of TLDs have been proven to be exceptionally reliable in industry for dosimetry, alternate means of measurement can corroborate current methods of detection. The purpose of this thesis is to provide the groundwork for an alternate radiation detection monitoring system with a dosimetry method in real time using commercially available silicon PIN diodes.

B. GOALS

The primary goal of this research project was to measure the effective radiation dosage of the NPS Flash X-ray facility using silicon PIN diodes. The results were compared to the dose readings of TLDs at increasing distances to correlate the output readings of the PIN diodes. The investigation compared which technique either peak amplitude or waveform integral would provide closer correlation to TLD measurements.

C. BENEFITS

Accurate radiation measurement at NPS Center for Radiation Hardened Electronics would greatly improve research in the area of space-based electronics. By using the PIN diodes as radiation detectors, this would possibly allow real time detection monitoring at the Flash X-ray facility. This can also be used to correlate TLD readings to verify dose amount during experimentation. Research conducted in this project can also provide information for continued study at the NPS electron linear accelerator facility (LINAC).

D. THESIS OVERVIEW

This thesis is divided into five chapters. Chapter I introduces the purpose, goals, and benefits of this thesis. Chapter II provides theoretical background about radiation

and dosimetry theory and semiconductor device operation. Chapter III provides explanation of the experiment conducted. Chapter IV presents a detail analysis of the results. Chapter V summarizes the conclusion reached and provides recommendation and details where further research should be directed.

II. THEORETICAL BACKGROUND

This chapter describes radiation, its sources and interactions. Also a brief explanation of semiconductor physics and how a photodetector works are provided.

A. RADIATION AND DOSIMETRY THEORY

Radiation can be categorized into two general types, charged particle radiation, which consists of fast electrons and heavy charged particles, and uncharged particles, which include electromagnetic radiation and neutrons [Ref. 1]. Radiation of concern with this thesis is electromagnetic radiation or short wavelength photons which includes X-rays emitted in the rearrangement of electron shells of atoms or charged particle collisions and gamma rays which originate from interaction within the nucleus. The ways these photons interact with matter are identical. They are lightly ionizing, highly penetrating and do not displace the material irradiated. Ionization is the creation of electron–hole pairs in a material by incident radiation. Ionization produces energetic charged particles through Coulombic interactions by completely removing electrons from the atom in the irradiated material. Generally, gamma and X-rays photons interact in this manner. The energy range of X-rays span approximately over four decades, ranging from about 0.1 eV to 1 MeV, while gamma rays range from about 10 keV to 100 MeV. Energies greater than 100 eV are usually called high energy electromagnetic radiation. Energies emitted from the NPS Flash X-ray facility are approximately 1.5 MeV.

X-ray produced in the NPS Flash X-ray facility is a result of the bremsstrahlung process. Bremsstrahlung is a German term, “brems” meaning braking or deceleration and “strahlung” meaning radiation. This process occurs when a negatively charged electron in motion is deflected by the positively charged atom nuclei. The deflection of electrons involves the loss of kinetic energy or velocity. The resultant energy loss generates electromagnetic radiation or X-rays [Ref. 1].

1. Energy and Dose Rate

The electron volt is used for radiation because the energy gained from an electric field can be found by multiplying the potential difference by the number of charges carried by a particle. The SI unit of energy is joule (J). Radiant energy can be converted to electron volt using

$$1 \text{ eV} = 1.602 \times 10^{-19} \text{ J}. \tag{2.1}$$

The energy of an X- or gamma ray photon is related to the radiation frequency by

$$E = h\nu, \tag{2.2}$$

where h is Planck's constant (6.626×10^{-34} J·s, or 4.135×10^{-15} eV·s) and ν is frequency. The wavelength λ is related to the photon energy by

$$\lambda = \frac{1.240 \times 10^{-6}}{E}, \tag{2.3}$$

where λ is in meters and E is in eV.

X-ray exposure is defined as the charge dQ due to ionization created by electron-hole pairs in a volume of air and mass dm. Therefore, the exposure value is dQ/dm with units of coulomb per kilogram (C/kg). Historically, Roentgen (R) defined exposure as the generation of one electrostatic unit of charge (about 2.08×10^{9} ion pairs) per 0.0001293 g (1 cm^3 at STP) of air [Ref. 2]. The two units are related by

$$1 \text{ R} = 2.58 \times 10^{-4} \text{ C/kg}. \tag{2.4}$$

Two different materials subjected to the same exposure will absorb different amounts of energy. Therefore, the energy absorbed from any type of radiation is defined as the absorbed dose. Historically the unit of absorbed dose has been the rad. One rad creates 3.2×10^{13} electron–hole pairs in one gram of irradiated silicon. The SI equivalent is gray (Gy) defined as 1 joule/kilogram. The two units are simply related by

$$1 \text{ Gy} = 100 \text{ rad}. \tag{2.5}$$

Measurements have determined that the absorbed dose in air corresponding to X-ray exposure of 1 coulomb/kilogram is equivalent to 33.8 joules/kilogram or 33.8 Gy [Ref. 1]. Total dose is the integral of dose rate, the accumulation of ionization energy absorbed in a material [Ref. 2].

Conversion between dose and fluence is helpful in interpreting measurement in detectors. Fluence is defined as

$$\Phi = \frac{dN}{da}, \tag{2.6}$$

where dN represents differential number of particles that are incident on a sphere with differential cross-sectional area da. Directed fluence can be estimated by $\Phi = N/4\pi d^2$ where N is the number of particles emitted by a source and d is the distance from the source. Energy fluence is defined as

$$\Psi = \frac{dR}{da}, \tag{2.7}$$

where dR is the radiant energy on a sphere of cross–sectional area da. For a monoenergetic beam,

$$\Psi = \Phi \cdot E, \tag{2.8}$$

where E is the amount of energy.

The energy of a photon is imparted to a material in two–stage process. In the first process, photon energy transfers to electrons or charged particles. This is called kerma which is the acronym for kinetic energy released per unit mass. Kerma is defined as

$$K = \frac{dE}{dm}, \tag{2.9}$$

where dE is the sum of the initial kinetic energies of all charged particles freed by uncharged particles in a mass dm. The unit of measurement for kerma is gray (i.e., $\mathrm{J/kg}$) [Ref. 1]. The second process is where energy is being transferred to a material through ionization. Linear Energy Transfer (LET) is a measure of how energy is transferred from radiation to an exposed material as a function of distance. The integral of LET over a particle's range in a material is the total deposited energy. The unit for LET is $\mathrm{MeV \cdot cm^2/g}$ which can be multiplied by a material density to determine the energy per unit length. Another term for LET is mass collision stopping power (S/ρ) where S is the rate of energy loss per unit path length (dE/dx) and ρ is the density of the material. The unit for mass collision stopping power is also $\mathrm{MeV \cdot cm^2/g}$.

2. Interactions

There are three main interaction mechanisms that take part in radiation measurements: photoelectric absorption, Compton scattering and pair production. All of these processes lead to the partial or complete transfer of X-ray photons to electron energy.

The photoelectric process is the predominant mode of interaction for X-rays of relatively low energy (< 200 keV). Photoelectric absorption is the interaction in which the incident photon is absorbed in one of the electron shells of the atom. The photoelectron is the kinetic energy given by the incident photon energy hv minus the binding energy of the electron in its original shell (E_b)

$$E_{e-} = hv - E_b. \tag{2.10}$$

This process is also improved for absorbent materials of high atomic number, Z, because the probability of photoelectric absorption per atom is approximately proportional to Z^5 [Ref. 1].

Compton scattering takes place between the incident photon and an electron in the absorbing material. This interaction is illustrated in Figure 1. The incoming photon is deflected at an angle by an electron at rest know as the recoil electron.

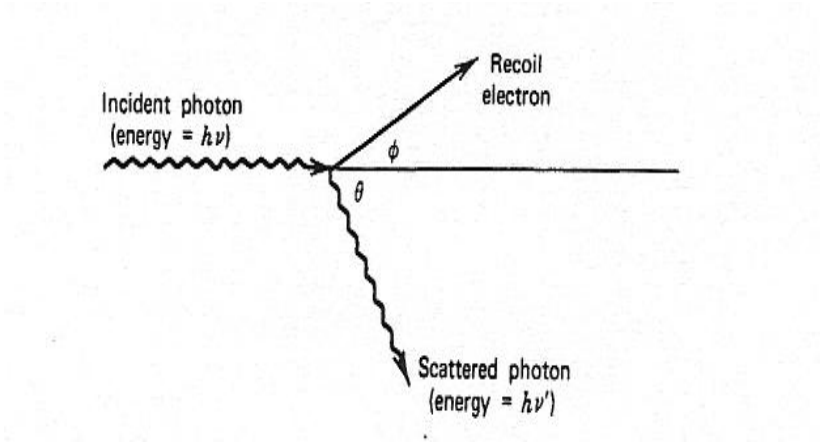

Figure 1. Compton scattering [From Ref. 1.].

This mechanism is expressed in the equation

$$hv' = \frac{hv}{1 + \frac{hv}{m_0 c^2 (1 - \cos\theta)}}, \tag{2.11}$$

where $m_0 c^2$ is the rest-mass energy of the electron (0.511 MeV). Varying angles of scattering are possible, therefore the energy transferred can vary. This interaction is expressed by equations for conservation of energy and momentum. It is the predominant interaction mechanism for energies of radioisotope sources. The probability of Compton scattering per atom of the absorbent material depends on the number of electrons available and therefore increase linearly with Z.

The third significant interaction is pair production. This occurs when incident photon is absorbed and creates an electron–positron pair. Since the rest-mass of an electron–positron pair is 0.511 MeV, the minimum energy required to create the pair is 1.02 MeV. The excess energy appears in the form of kinetic energy shared by the electron–positron pair, which total

$$E_{e-} + E_{e+} = hv - 2m_0 c^2. \tag{2.12}$$

There is no expression for the probability of pair production per nucleus, but the magnitude varies approximately as the square of the absorber atomic number. Figure 2 illustrates all three major X-ray interactions in given material.

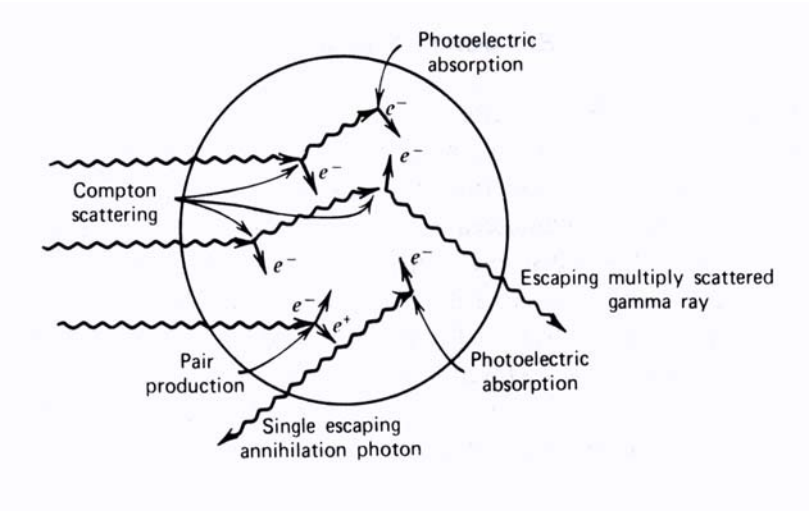

Figure 2. Illustration of the three major interactions [From Ref. 1.].

The importance of the three interactions is illustrated in Figure 3. The line at the left represents the energy at which photoelectric absorption and Compton scattering are

equally probable as a function of the absorber atomic number. The line at the right represents the energy at which Compton scattering and pair production are equally probable. Silicon (Z=14) is shown to determine which of the three interaction has the dominant affect as a function photon energy.

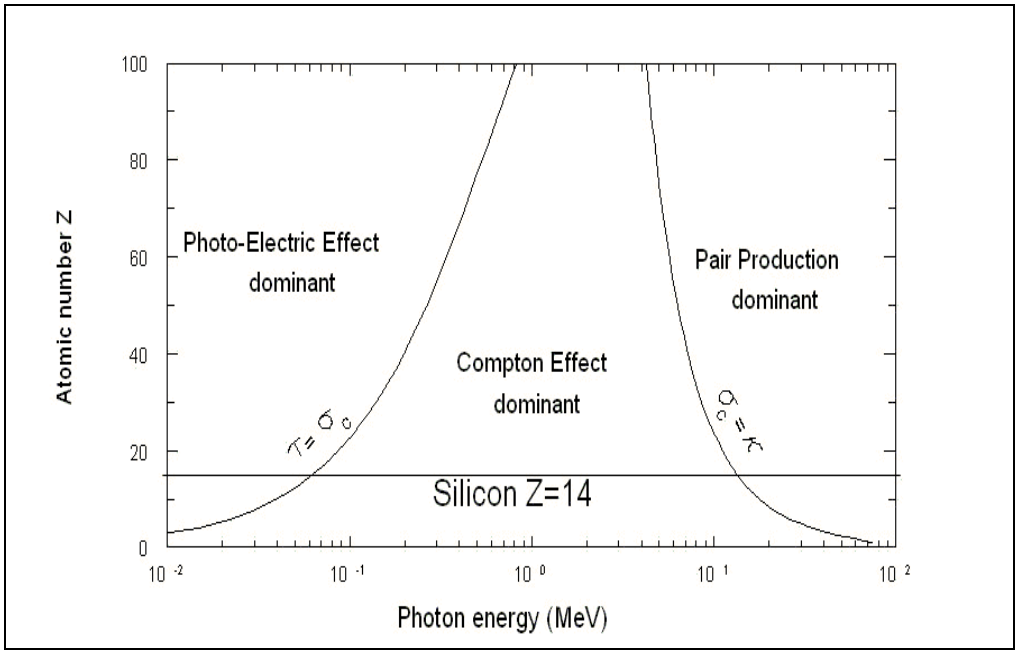

Figure 3. Relative importance of the three types of X-ray interactions [After Ref. 3.].

3. Attenuation

One important feature of electromagnetic radiation that must be considered is the variation in attenuation and absorption of different materials. These interactions can be characterized by a fixed probability of occurrence per unit length in the absorber. It is often a misnomer of these two terms. Attenuation is the decrease in intensity of a beam as a result of energy absorption. Absorption is the transfer of photon energy to the absorbing material. The sum of these probabilities is called linear attenuation coefficient, μ, and is the probability per unit path length

$$\mu = \tau(\text{photoelectric}) + \sigma(\text{Compton}) + \kappa(\text{pair}). \tag{2.13}$$

The intensity of the radiation after and before it passes through an absorber is I and I_0, and

$$I = I_0 e^{-\mu/\rho d}, \tag{2.14}$$

where d is the thickness of the absorber and ρ represents the density of the medium.

Mass attenuation coefficient (μ/ρ) measures the deflection of monoenergetic photons of a material. Mass energy absorption coefficient (μ_{en}/ρ) takes into account of the secondary charged particles produced in a form of energy loss [Ref. 4]. Figure 4 shows the mass attenuation coefficient and the mass energy absorption coefficient as a function of photon energy for Silicon (Z=14). Figure 5 displays the mass energy coefficient and mass collision stopping powers for air and material of interest in radiation hardness testing: Lithium Fluoride (LiF), Calcium Fluoride (CaF_2), Aluminum (Al) and Silicon (Si).

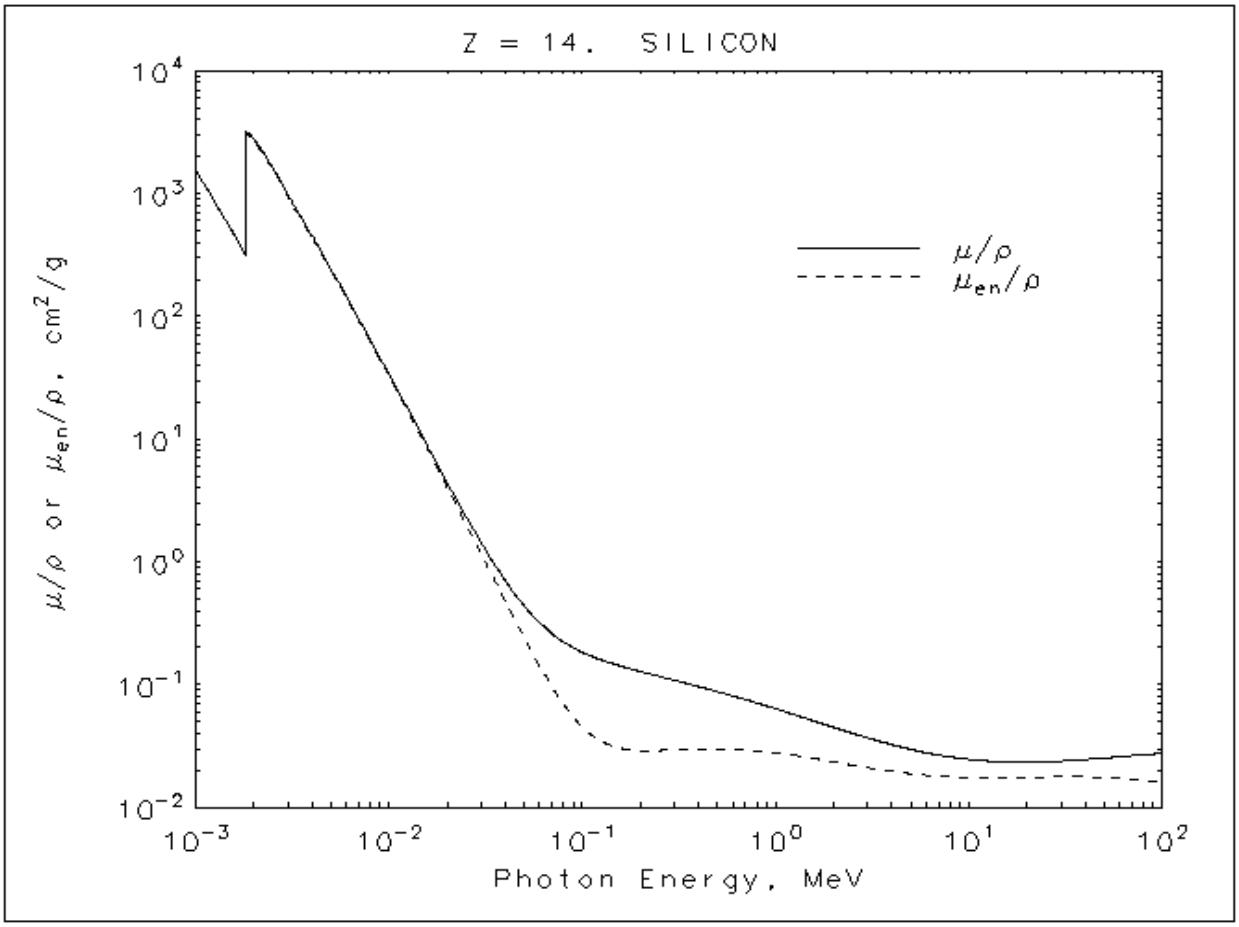

Figure 4. Values of the mass attenuation coefficient, (μ/ρ), and the mass energy-absorption coefficient, (μ_{en}/ρ), as a function of photon energy, for Silicon, Z=14 [From Ref. 4.].

Energy, MeV	Air		LiF		CaF_2		Al		Si	
	μ_{en}/ρ	S/ρ	μ_{en}/ρ	S/ρ	μ_{en}/ρ	S/ρ	μ_{en}/ρ	S/ρ	μ_{en}/ρ	S/ρ
0.01	4.64	19.8	5.61	18.0	48.0	16.7	25.0	16.5	32.4	16.9
0.02	0.526	11.6	0.635	10.6	6.62	9.94	3.06	9.84	4.01	10.1
0.04	0.0669	6.85	0.0774	6.25	0.832	5.97	0.356	5.91	0.473	6.07
0.06	0.0300	5.11	0.0318	4.67	0.249	4.49	0.109	4.44	0.142	4.56
0.08	0.0239	4.20	0.0237	3.84	0.113	3.70	0.0546	3.66	0.0684	3.76
0.1	0.0232	3.63	0.0222	3.32	0.0670	3.21	0.0377	3.18	0.0449	3.26
0.2	0.0267	2.47	0.0248	2.26	0.0311	2.20	0.0274	2.18	0.0290	2.24
0.4	0.0295	1.90	0.0273	1.74	0.0294	1.71	0.0286	1.68	0.0297	1.73
0.6	0.0295	1.74	0.0274	1.58	0.0289	1.56	0.0285	1.54	0.0295	1.58
0.8	0.0288	1.68	0.0267	1.52	0.0281	1.51	0.0278	1.49	0.0287	1.53
1.0	0.0279	1.66	0.0258	1.49	0.0271	1.48	0.0268	1.47	0.0278	1.51
2.0	0.0234	1.68	0.0217	1.47	0.0229	1.48	0.0226	1.48	0.0234	1.52
4.0	0.0186	1.79	0.0173	1.51	0.0192	1.53	0.0188	1.54	0.0196	1.59
6.0	0.0164	1.87	0.0153	1.55	0.0180	1.58	0.0174	1.58	0.0182	1.64
8.0	0.0152	1.93	0.0141	1.57	0.0175	1.61	0.0167	1.61	0.0177	1.67
10	0.0145	1.98	0.0134	1.59	0.0174	1.64	0.0164	1.64	0.0175	1.70
20	0.0131	2.13	0.0122	1.65	0.0176	1.71	0.0164	1.71	0.0176	1.77
40	0.0124	2.28	0.0119	1.71	0.0181	1.77	0.0168	1.77	0.0182	1.84
60	0.0122	2.35	0.0116	1.74	0.0177	1.81	0.0165	1.80	0.0178	1.87

Figure 5. Mass energy absorption coefficients: μ_{en}/ρ (cm^2/g) and mass collision stopping powers: S/ρ ($\mathrm{MeV}\cdot\mathrm{cm}^2/\mathrm{g}$) for several material of interest in radiation hardness testing [From Ref. 5.].

Figures 6 and 7 are the graphical representation of the ratios of mass energy absorption coefficient and mass collision stopping power of Silicon to air and materials of interest in radiation hardness testing [Ref. 5]. The figures show the reasonable absorption characteristics that CaF_2 shares with Silicon of energies greater that 1 MeV.

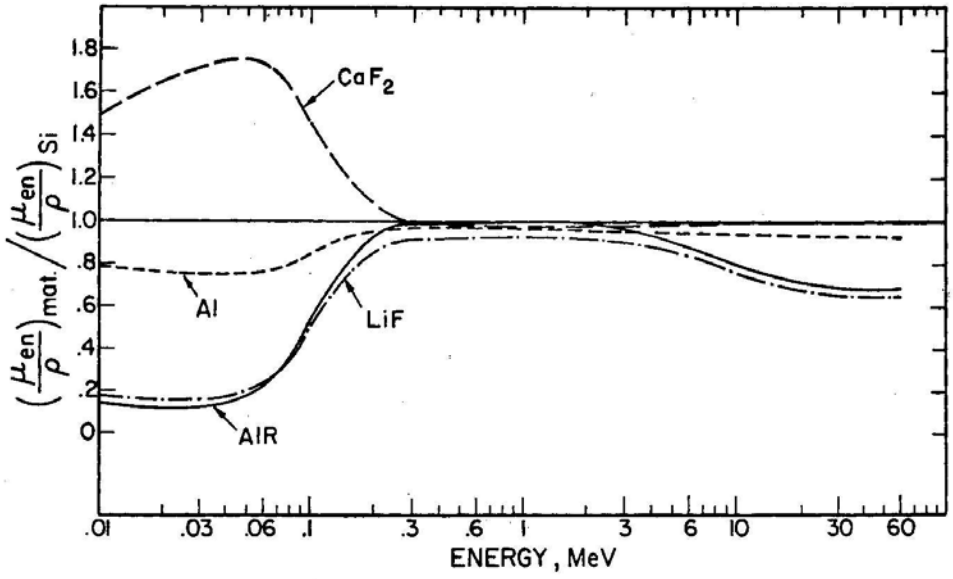

Figure 6. Ratios of mass energy absorption coefficients of various materials relative to Silicon [From Ref. 5.].

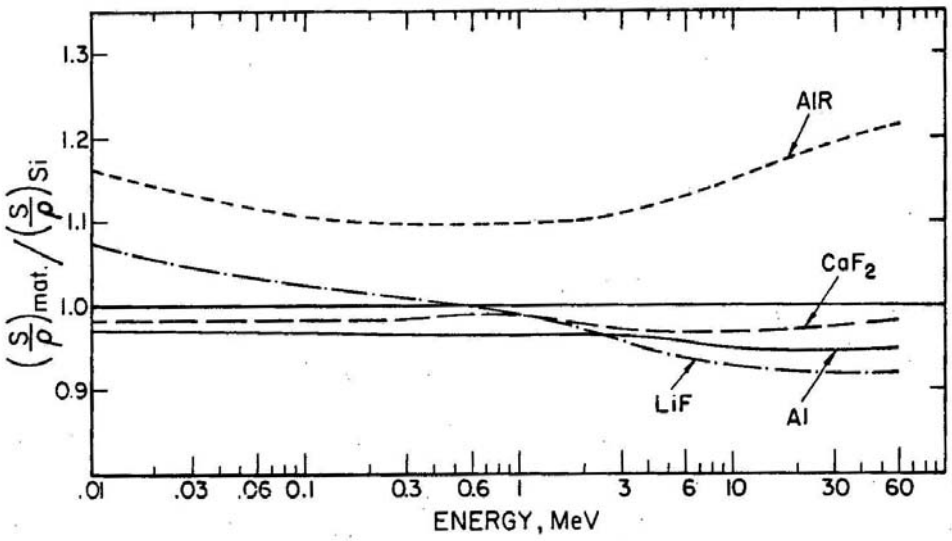

Figure 7. Ratios of mass collision stopping powers of various materials relative to Silicon [From Ref. 5.].

B. RADIATION DETECTION DEVICES

The semiconductor diode has been the primary choice of radiation detectors. High energy resolution can be obtain because of the large number of carriers that result from a given incident radiation event. Other desirable characteristics are relative fast time constant and small effective thickness. The only disadvantage is the possible degradation due to radiation damage to the semiconductor material. The most widely available choice of commercial semiconductor material for diodes is Silicon.

1. Semiconductor Physics

A semiconductor has a periodic lattice structure crystal that allows energy bands for electrons to exist. The energy of any shared electron within the pure material must be confined to one of these energy bands that are separated by gaps. This forbidden gap is bounded by the valence band which corresponds to the outer shell electrons. These electrons are covalently bonded to a specific lattice site in the crystal. The next higher band is called the conduction band which is the region where electrons are allowed to migrate freely. The two bands are separated by the bandgap which determines how the material is classified.

As electrons are excited out of the valence band, they leave a vacant space in the valence band called a hole. The hole can be considered as a moving positive charge and the free electrons as negative charge. These are called charged carriers. Under the influence of an applied electric field, electrons move throughout the conduction band, holes in the valence band. The carrier with the greater concentration is called the majority carrier and the carrier with lesser concentration is called the minority carrier. The combination of the two is called an electron–hole pair and the process is called generation. When electrons return to the valence band, it is called recombination. This annihilates the electron–hole pair. In an intrinsic material, a crystal free of impurities, an equal number of holes and free electrons exist. The number of electrons at the various energy levels is governed by the Fermi–Dirac distribution function. The higher the energy level, the greater the probability that an electron will occupy that level. The Fermi level is the energy level at which the probability of occupancy is fifty percent.

When an electric field is applied to the semiconductor material, both the electrons and holes will undergo migration. This movement is a combination of the random

thermal velocity and net drift velocity parallel to the direction of the applied field [Ref. 3]. An electron leaves one position to fill an existing hole and is being drawn in the opposite direction of the electric field. The hole moves in the same direction of the electric field. Therefore the velocity, v, for both electrons and holes can be defined by

$$v_h = \mu_h E, \tag{2.15}$$

$$v_e = \mu_e E, \tag{2.16}$$

where E is the electric field magnitude and μ is the electron or hole mobility. At higher electric field values, the drift velocity increases more slowly with the field. Eventually, saturation velocity is reached and velocity becomes independent of the further increases in the electric field. Semiconductor diode detectors operate at a high electric field in reverse bias to produce saturation velocity for the charged carriers [Ref. 6].

Imperfections in a crystal lattice structure may trap or recombine charge carriers and introduce new energy levels. An impurity atom with more valence electrons than its original configuration donates electrons to the conduction band is called the donor. Material containing donor impurities are known as n-type. An impurity atom with fewer valence electrons than its original configuration accepts electrons in its valence band, leaving holes, is called an acceptor. Material containing acceptor impurities are called p-type. These processes are called doping. These impurities produce energy levels that exist in the bandgap. These energy levels are called traps or recombination centers for the majority and minority carriers, causing them to annihilate.

When n-type and p-type materials are brought together, they form a pn junction. Since each type has a concentration of charge carriers, they will diffuse toward each other and create a region counteracting with an electric field. This region is called the depletion region and will extend on both the p- and n-sides. The buildup of net charge in the region will have an electric potential difference. The value at any point can be expressed as a Poisson's equation

$$\nabla^2 \varphi = -\frac{\rho}{\varepsilon}, \tag{2.17}$$

where ε is the dielectric constant of the medium, φ is the electric potential and ρ is the net charge density [Ref. 1]. Over distance x the equation is now

$$\frac{d^2\varphi}{dx^2} = -\frac{\rho(x)}{\varepsilon}. \tag{2.18}$$

The electric field, E, is expressed as

$$E(x) = -\frac{d\varphi}{dx}. \tag{2.19}$$

When a pn junction has an external bias or voltage applied, it will function as a diode. A forward biased diode is when a positive voltage is applied to the p-side of the junction with respect to the n-side. The electrons in the n-side will travel across the junction and holes on the p-side, therefore allowing current to conduct. When the diode is reverse biased, the p-side has a negative voltage and no current is flowing. The junction is acting as a rectifying element preventing the flow of majority carriers from each side [Ref. 6].

2. Basic Photodiode Operation

A semiconductor photodiode is a reversed-biased pn junction diode where the absorption of photons creates electron–hole pairs in the depletion region. The photogenerated carriers in the depletion region results in current flow caused by the electric field. The amount of energy required to create the electron–hole pair is the bandgap of the semiconductor material (E_g). The average energy necessary to create an electron-hole pair in silicon (Si) is ~3.6 eV. This average energy is about three times the forbidden gap energy (~1.1 eV) because energy and momentum must match the crystal band structure to continue in the absorption process. The photon energy associated with this phenomenon is expressed as $E_{\text{ph}} = h\nu$ where h is Planck's constant (6.626×10^{-34} J·s) and ν is the frequency of the electromagnetic wave. For photogeneration to occur, $h\nu$ has to be greater than or equal to the bandgap of the material. If photons are uniformly distributed throughout the junction, the amount of photocurrent produced is proportional to the number of electron–hole pairs generated.

3. PIN Diode

The PIN photodiode is a three region structure where an intrinsic region is placed between heavily doped p- and n-regions. The intrinsic layer is fully–depleted at zero or small reverse biases. The heavy doping of the p- and n-regions causes the depletion widths to be very narrow and the diffusion length of the minority carrier to be relatively small. This results in the greater part of the photocurrent to be generated from the carriers generated in the central depletion region [Ref. 6]. Figure 8 illustrates an incident photon creating an electron–hole pair in a PIN diode.

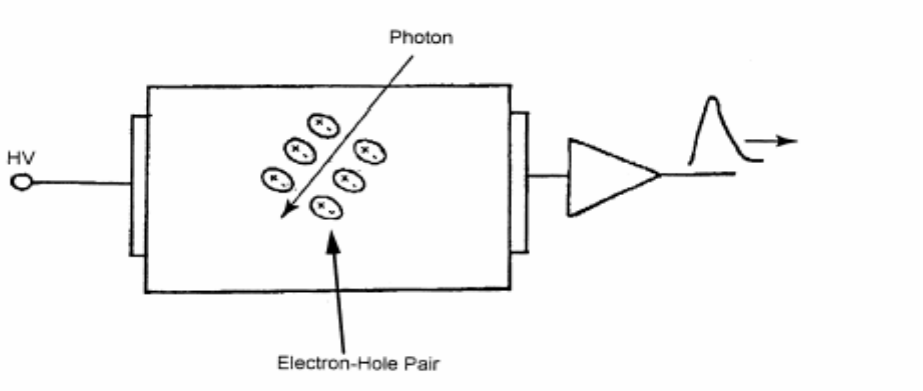

Figure 8. Schematic illustration of incident photon creating electron–hole pair in a diode [From Ref. 7.].

C. THERMOLUMINESCENT DOSIMETER (TLD)

The NPS Flash X-ray facility currently uses thermoluminescent dosimeters (TLDs) as its primary choice of radiation monitoring and detection. TLDs consist of inorganic scintillation materials that when exposed to ionizing radiation causes electron (and holes) to migrate and traps the charge (as shown in "A" in Figure 9). When read out, the scintillated photons are released when an electron–hole pair formed by an incident radiation recombined at an activator site. The material of choice utilized by the Flash X-ray facility for the TLDs are Manganese–doped Calcium Fluoride (CaF_2:Mn) which is designated TLD-400.

The thermoluminescent read–out process is further illustrated in "B" in Figure 9. Ionizing radiation elevates an electron to the conduction band where it is captured in an electron trap. This is where a place in the crystal lattice structure is missing a negative

ion. The hole left behind similarly migrates to a hole trap. The energy depth of theses traps coincide with the energy required for the particle to overcome the potential of the hole and is sufficient to prevent the escape of the electron at room temperature. Continued exposure of the material increases the number of electrons trapped. The material must be heated for readings. The light yield upon heating corresponds to the radiation exposure which is related to the number of radiated photons [Ref. 8].

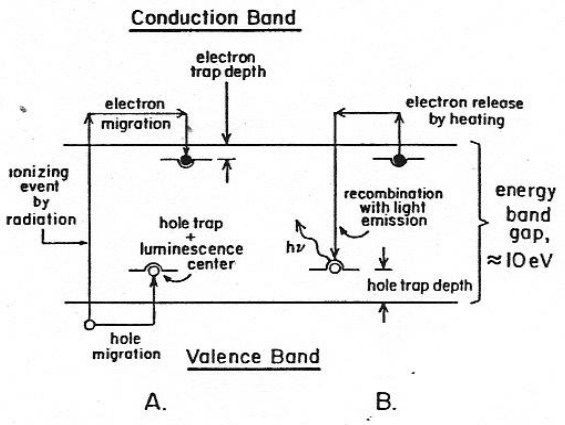

Figure 9. Energy level diagram of the thermoluminescent process [From Ref. 8.].

This chapter reviewed basic radiation and dosimetry theory and semiconductor device fundamentals. This will assist the reader in the following chapters and help in analyzing the results. Chapter III follows with a discussion on how the experiment was conducted, describes the equipment and device used in the experiment.

III. EXPERIMENT AND DATA COLLECTION

This chapter lists the equipment and devices used for the experiment. It also provides the layout of the circuit used for radiation detection and an explanation of the experiment.

A. EQUIPMENT

1. NPS Flash X-ray Facility

The NPS Flash X-ray facility is a Model 112A Pulserad X-Ray Generator installed in 1988 by the Physics International Company. High power X-ray radiation is produced in the series of three steps. A twelve–stage Marx Generator is charged via an external power supply to the desired voltage on the capacitor bank. The Marx Generator is a system which consists of a number of capacitors which are charged in parallel and discharged in series to produce high output voltages. The Blumlein Pulse Forming Line is then resonantly charged from the Marx Generator. The Blumlein is a transmission line that shapes the voltage pulse to a rectangular flat–top pulse and provides input/output impedance matching to a load. When fully charged, the Blumlein discharges rapidly into the electron accelerator tube creating a large potential difference across the diode gap. The cathode consists of a stainless steel rod which readily emits electrons when the high voltage is applied. The electrons are accelerated across the cathode–anode spacing until they impact with a tantalum foil target. The resulting bremsstrahlung process produces X-ray radiation. The charging and discharging phases of the operation are controlled through a triggering system. This triggering system consists of numerous gas spark gap switches whose closure is a result of the electrical breakdown of the pressurizing gas, sulfur hexafluoride [Ref. 8]. Figure 10 is a diagram of the Flash X-ray generator. A summary of the design specifications listed in the Operations and Maintenance Manual is provided in Table 1.

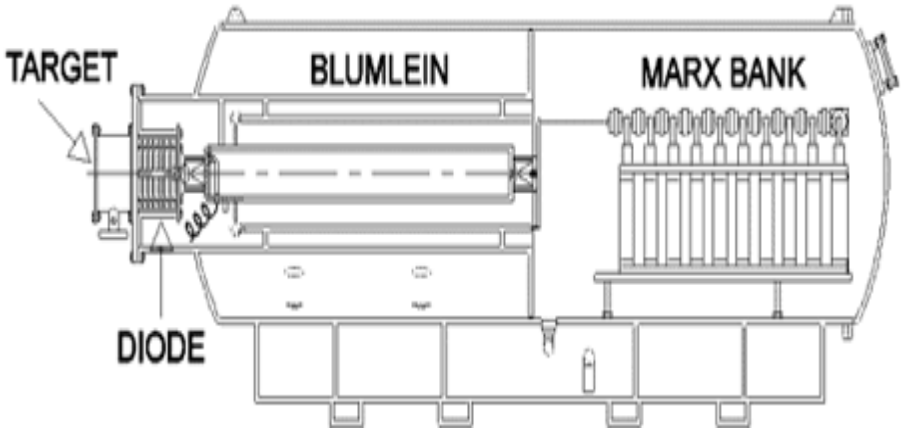

Figure 10. Diagram of Model Pulserad112A Flash X-ray generator [From Ref. 8.].

X-ray Output	
Beam Dose	1 krad(Si)
Dose Rate	5×10^{11} rad/sec on 1 cm^2 area
Pulse width	10 ns
Coaxial Blumlein Pulse Forming Line	
Output Impedance	43 Ohms
Peak Output Voltage	1.2 MV
Marx Generator	
Number of Stages	12
Stage Capacitance	0.05 μF
Maximum Charge Voltage	100 kV

Table 1. Model 112A Pulserad X-ray Generator Specifications [After Ref. 8.].

2. SEMICOA SCA001C Silicon PIN Photodiode

The SEMICOA SCA001C is a commercially available silicon PIN photodiode. The total physical dimension of the chip used in the SCA001C is a square of side length of 0.05 inch (1.27 mm). The active area is 0.04 inch (1.02 mm) diameter with a thickness of 0.015 inch (0.381 mm) . The chip is hermetically sealed in a TO-18 metal case which is electrically isolated from the anode and cathode. Figure 11 provides an overview of the SEMICOA SCA001C photodiode. Appendix A includes the data and specification sheet provide by SEMICOA Semiconductors, Inc.

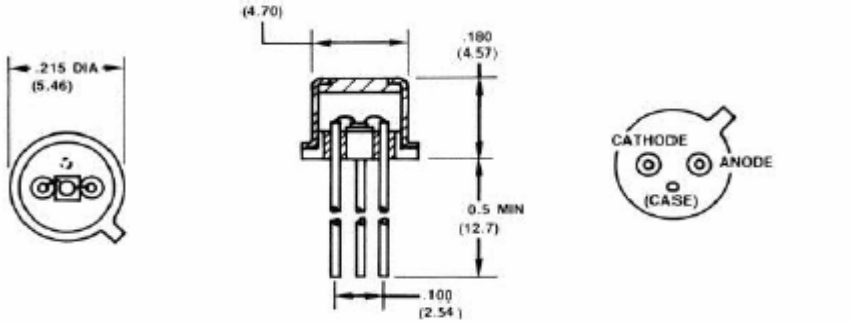

Figure 11. SEMICOA SCA001C mechanical specification view [From Ref. 9.].

B. CIRCUIT LAYOUT AND EXPERIMENT

PSPICE model and layout was used initially to simulate the circuit prior to testing. The following describes the circuit design and procedure for testing.

1. Circuit Design

The PIN diode was modeled as an independent current source placed in parallel with shunt resistance, series resistance and diode characteristics provided in the specification sheet. The independent current source represents the output pulse width of the flash X-ray. A ceramic capacitor was placed at the cathode to match the supply voltage of the PIN diode load. The RG-58 coaxial cable was modeled as a lossy transmission line because of the length of cable between the device and the measuring equipment was approximately to be 100 ft. A positive DC voltage source was placed at the cathode of the PIN diode through the coaxial cable to provide reverse biasing. A 50-Ohms termination resistance and input capacitance of 1 nF represented the input impedance of the measuring oscilloscope. Figure 12 shows schematic of test circuit. Figure 13 displays result of the PSPICE circuit simulation.

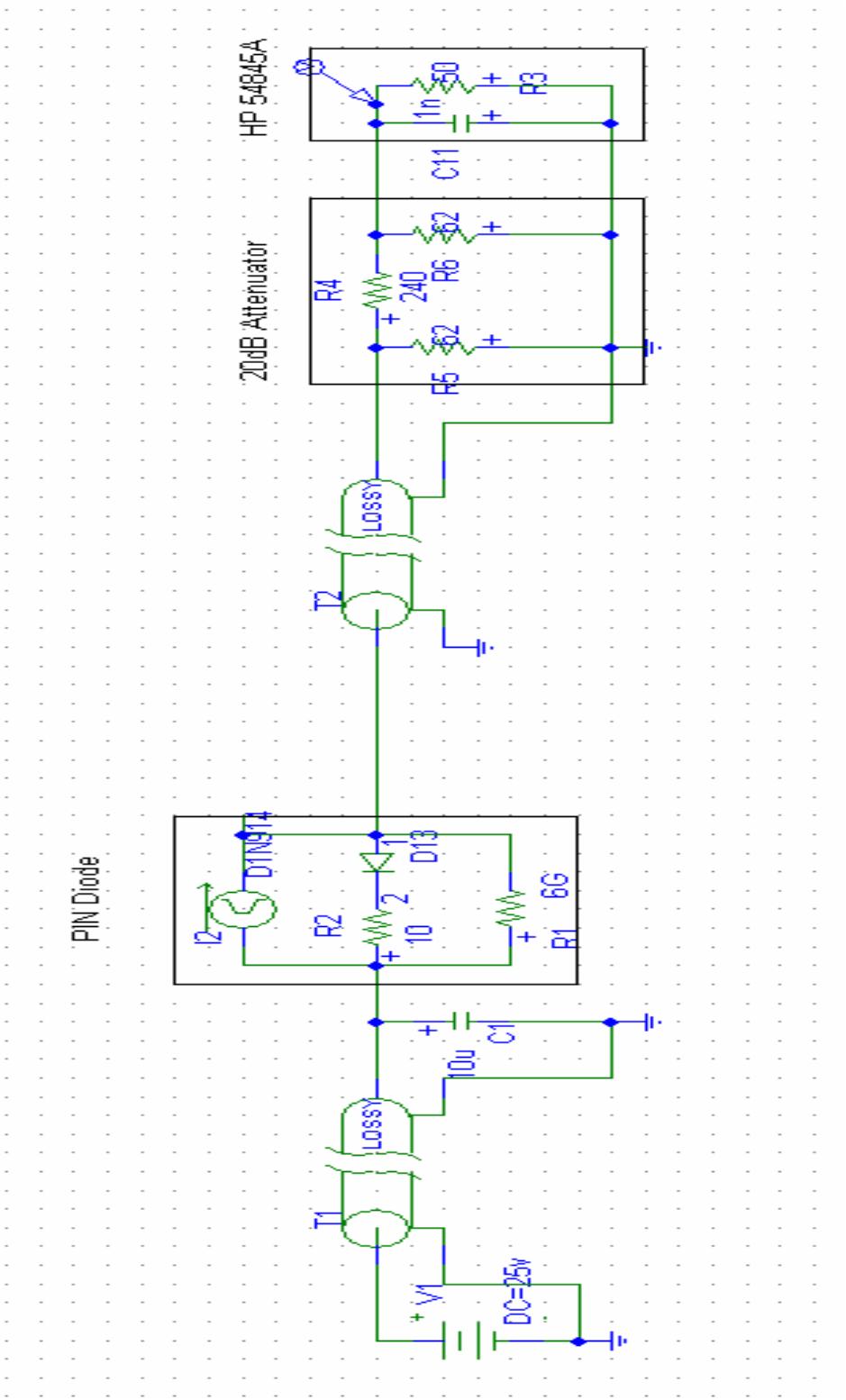

Figure 12. PSPICE schematic of test circuit.

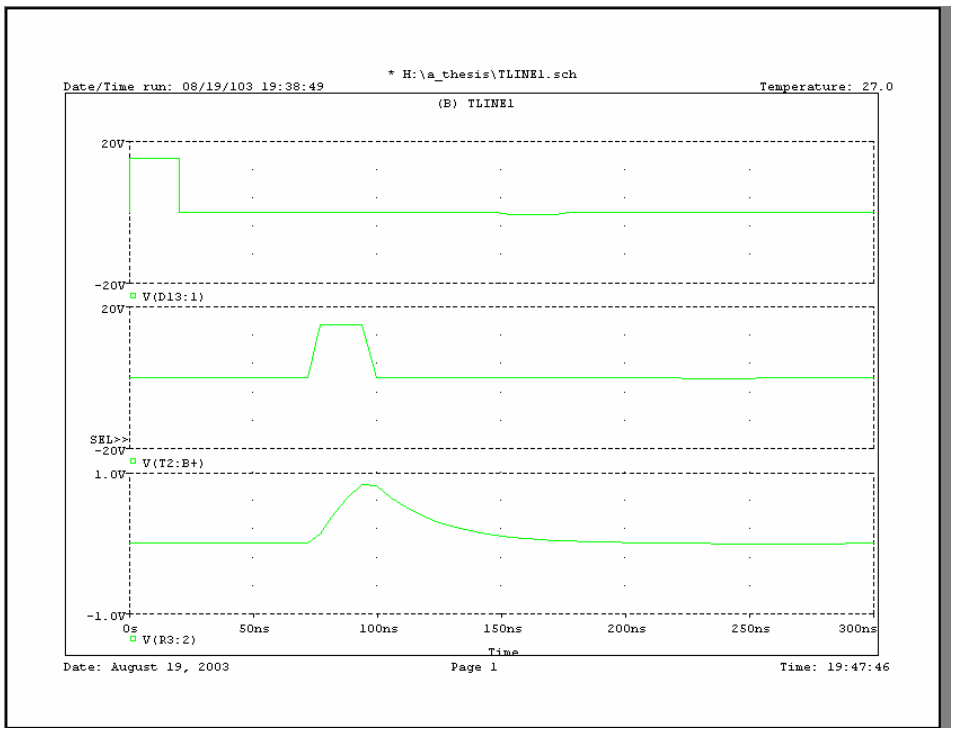

Figure 13. PSPICE predicted voltage output waveform.

The top voltage waveform in Figure 13 is the initial pulse from the diode. The middle waveform is the pulse after it has traveled through the transmission line. The lowest waveform is the pulse that is expected at the oscilloscope.

2. Circuit Test Procedure

The PIN diode test circuit was constructed on a perforated circuit board. The device was placed at varying distances at the anode end of the Flash X-ray generator. The coaxial cable provided voltage to the device under test and transported the signal to the measuring equipment. The PIN diode was reverse biased to 25 VDC, within the range to minimize the diode junction capacitance. A 20-dB attenuator was placed at the scope termination to reduce the signal on the display. The measuring oscilloscope, Hewlett Packard 54845A, captured the waveform of each shot. Dosimetry was performed by placing unshielded manganese-doped calcium fluoride (CaF_2:Mn) TLDs within 1 cm adjacent to the PIN diode during each shot. Since the TLD was placed close to the diode, beam uniformity and exposure across both devices were essentially equal. The dosage readings of the TLDs were conducted by a Victoreen Model 2800M TLD reader. The Flash X-ray facility operated at an approximate 85-kV Marx charge voltage for all test shots.

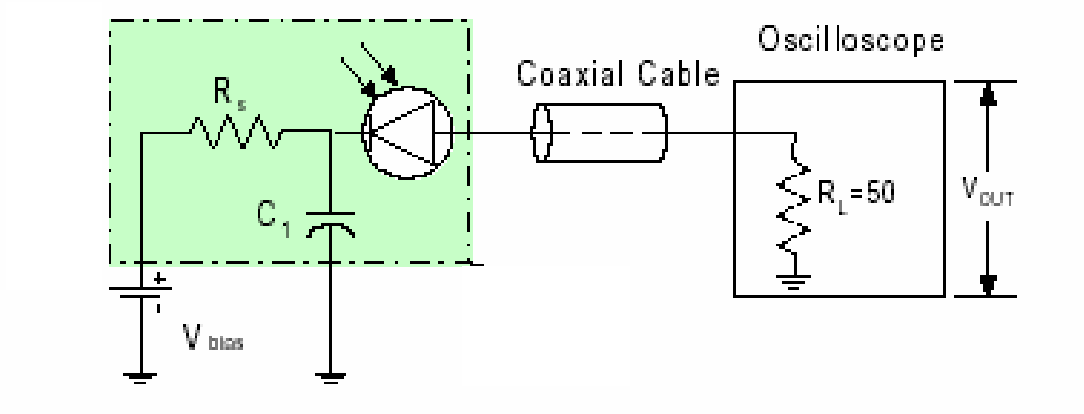

Figure 14. Schematic overview of test circuit [After Ref. 1.].

Figures 15–20 are the measured output waveforms at increasing distances. Detailed analyses of voltage waveforms are provided in Chapter IV.

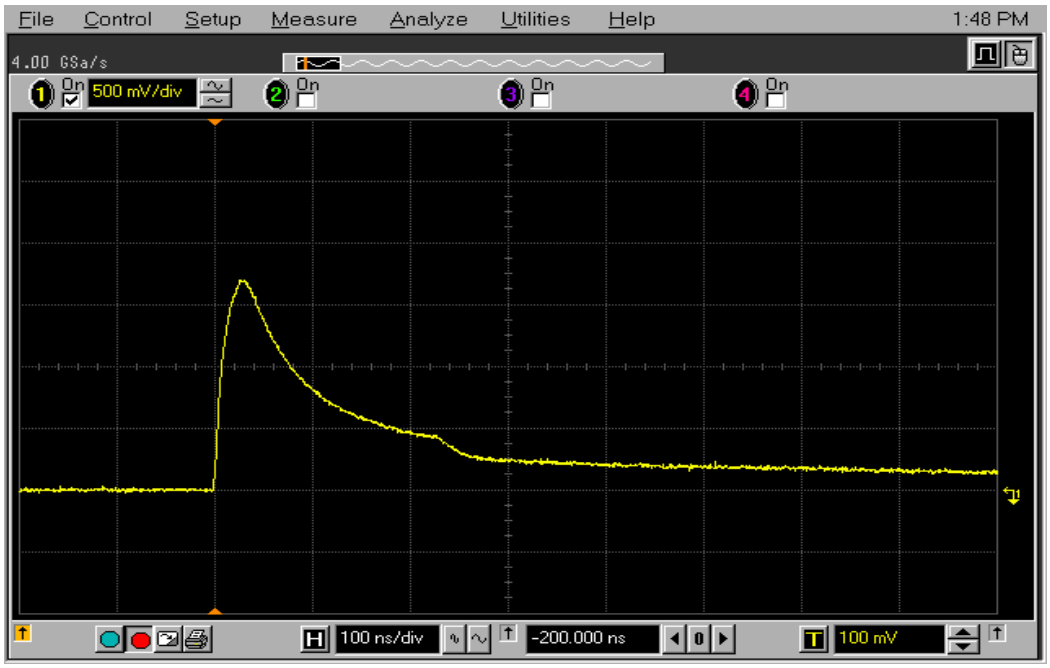

Figure 15. Photodiode waveform at 3 cm, peak voltage 1.80 V

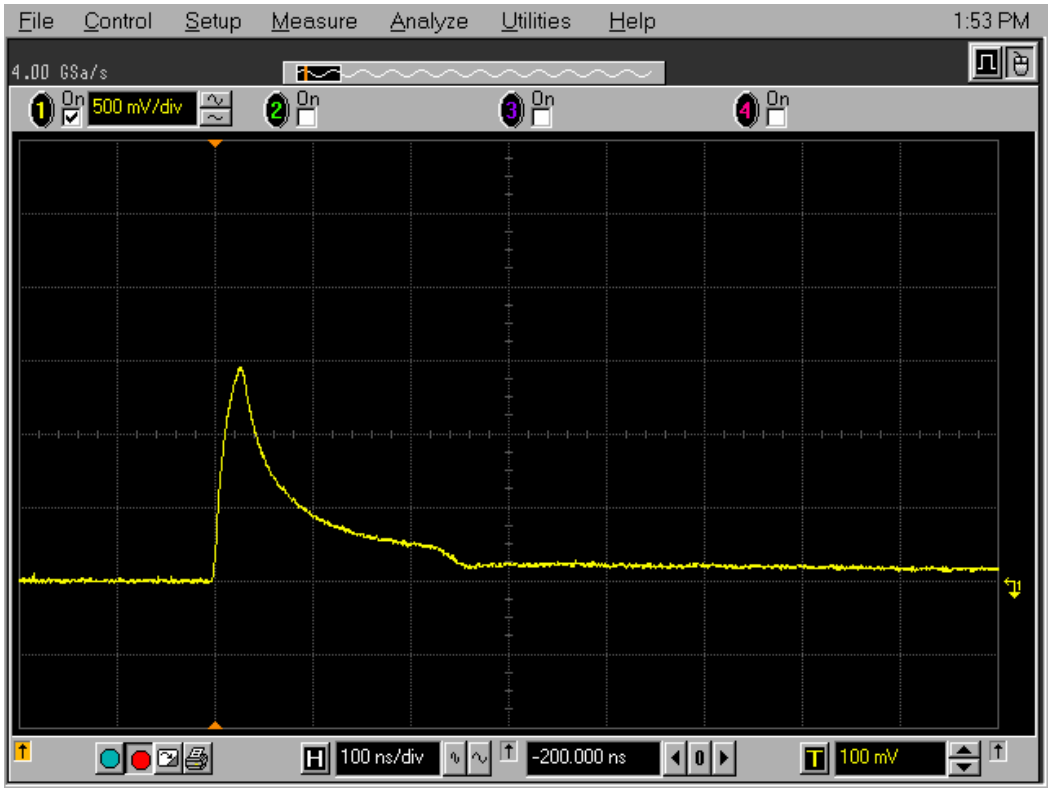

Figure 16. Photodiode waveform at 6 cm, peak voltage 1.50 V

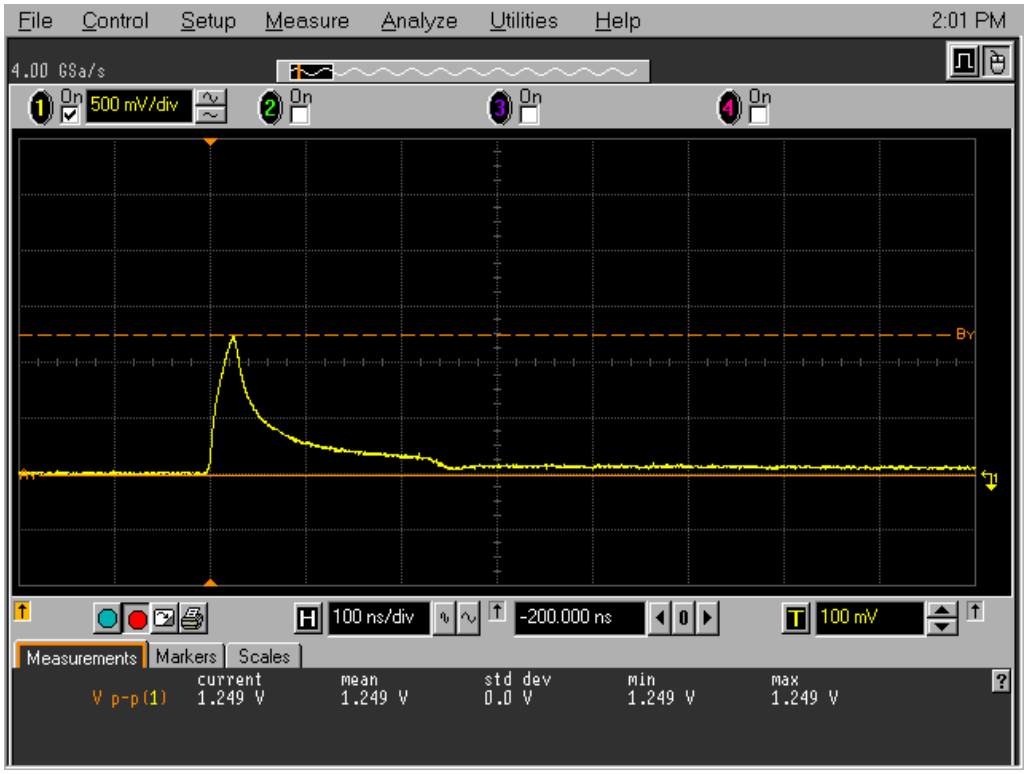

Figure 17. Photodiode wave form at 9 cm, peak voltage 1.25 V

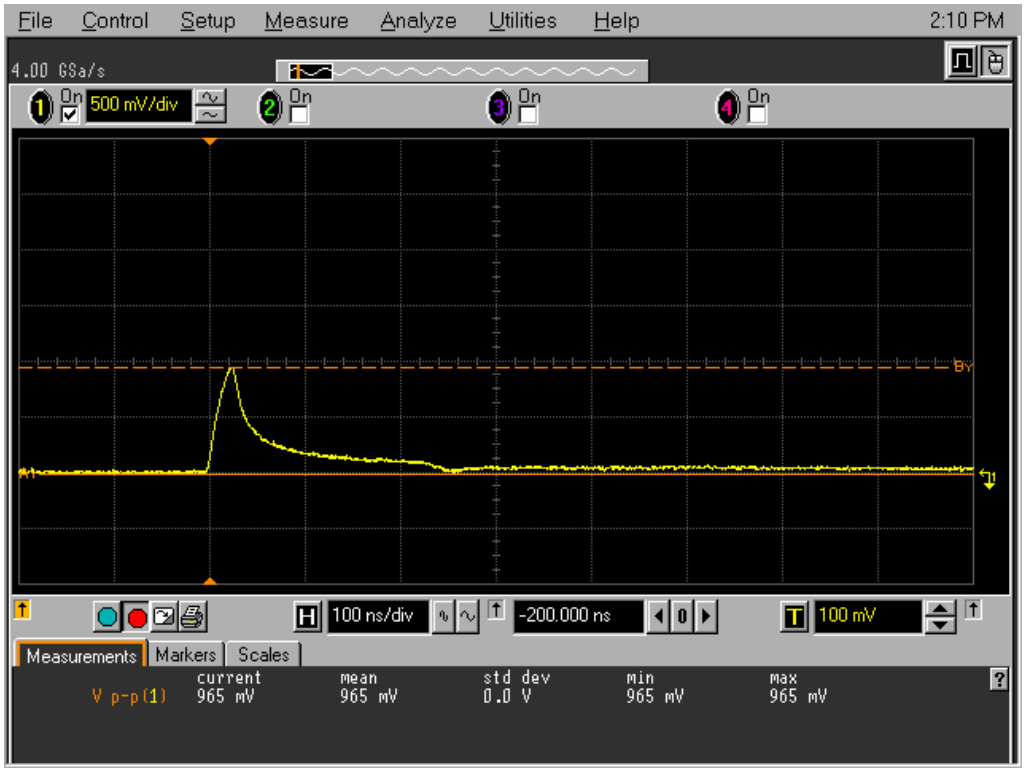

Figure 18. Photodiode waveform at 12 cm, peak voltage 0.98 V

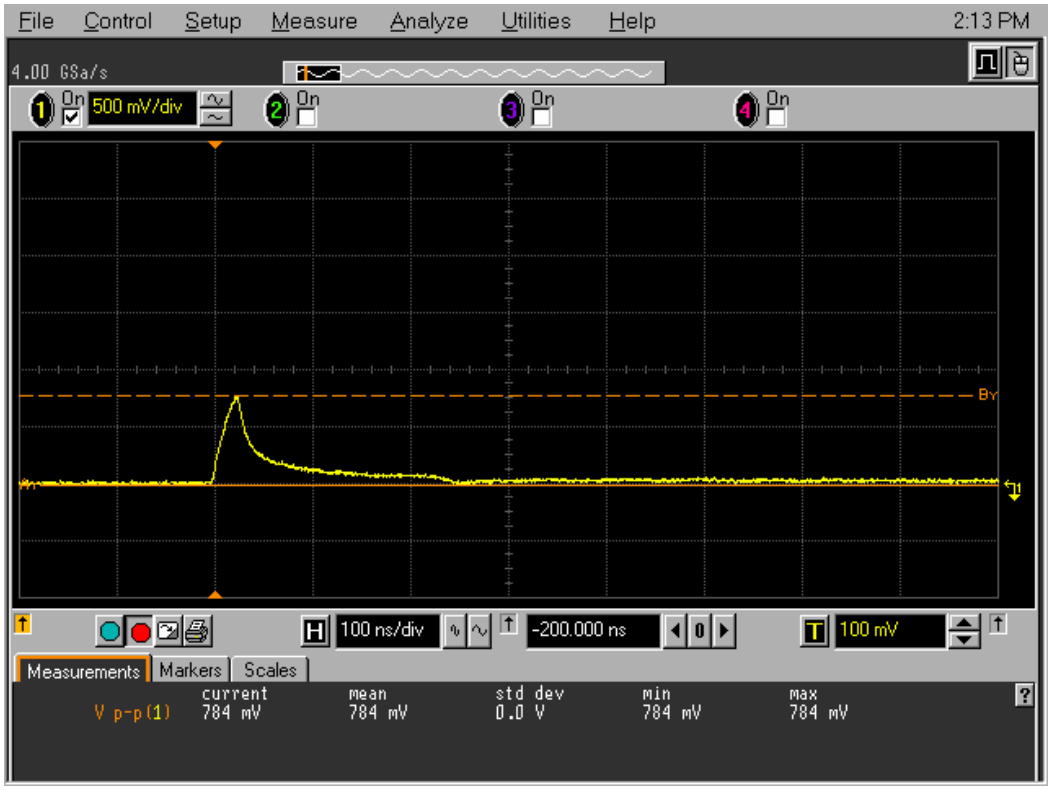

Figure 19. Photodiode waveform at 15 cm, peak voltage 0.78 V

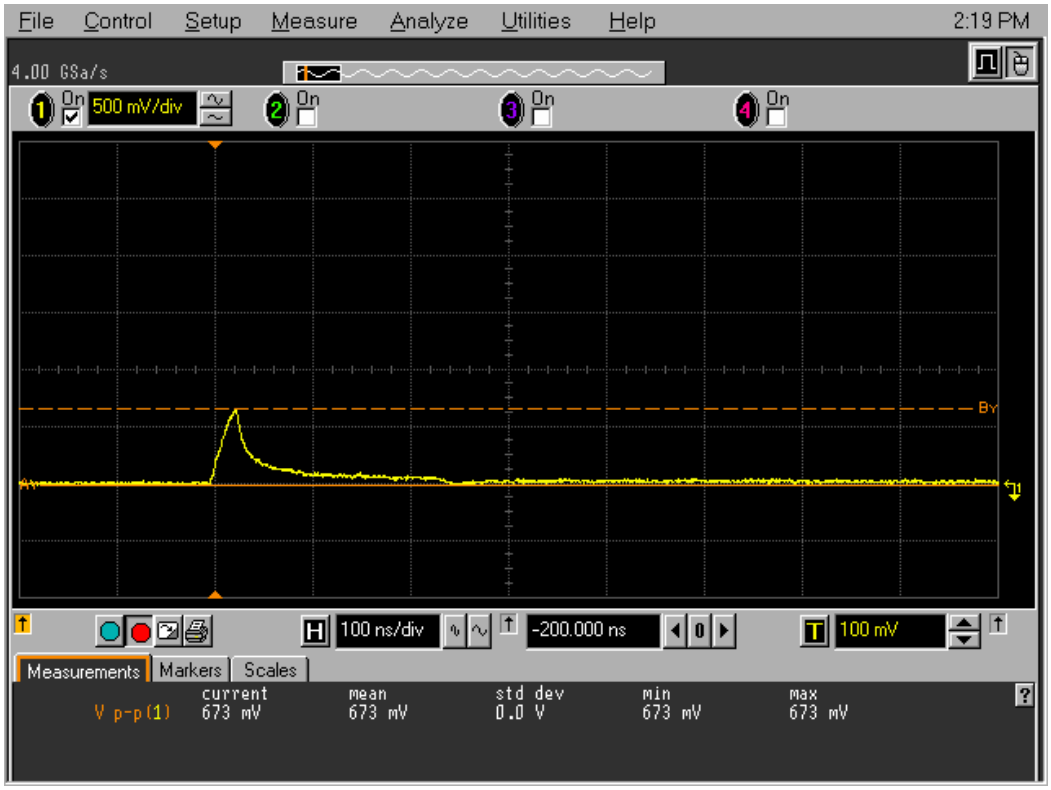

Figure 20. Photodiode waveform at 18 cm, peak voltage 0.67 V

3. Transfer of Energy

It is important to have an understanding of how the energy transformation takes place in the experiment. Even though the Flash X-ray facility initially produces a large amount of energy, only a small fraction can be captured and analyzed. As energy is being generated and transmitted by the Flash X-ray facility, energy is being transformed from radiative to electrical energy as it is being absorbed by the two detection devices. Losses occur at each transition point as it is being transferred and transformed. Figure 21 shows the approximate amount of energy being transferred and where the energy loss occurs.

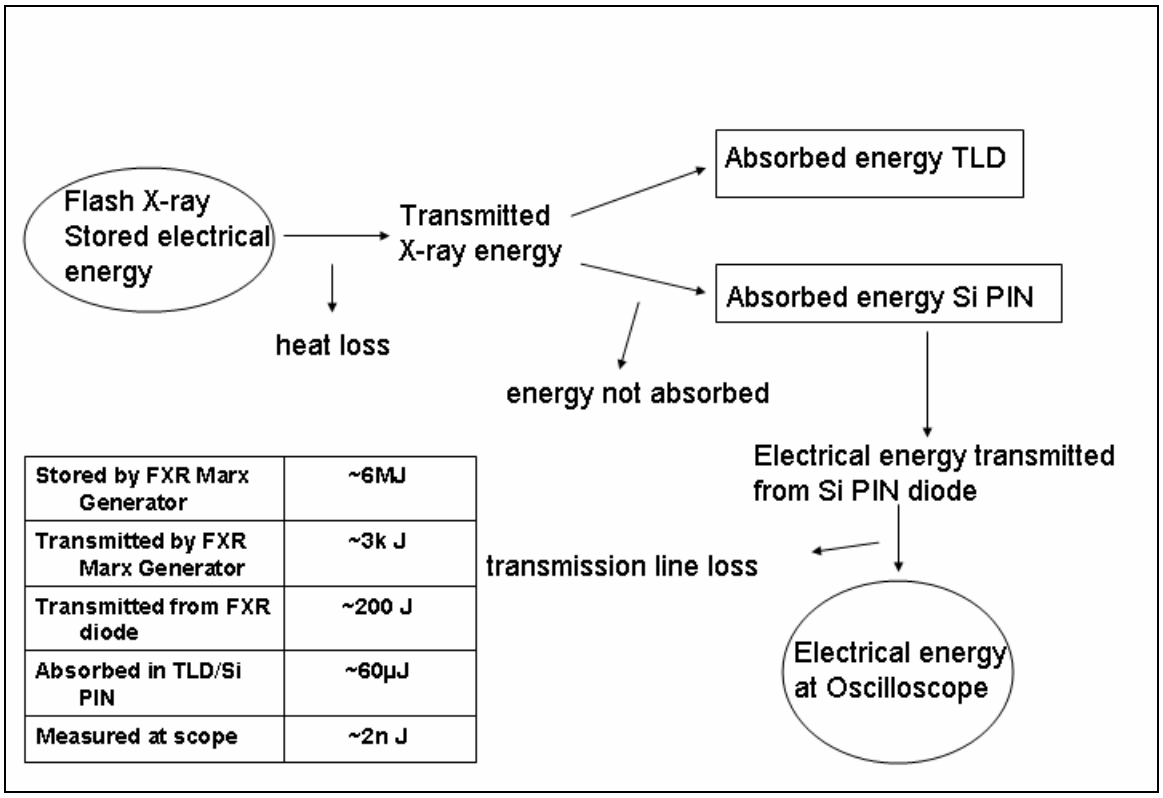

Figure 21. Diagram illustrating the transfer of energy in radiation measurement of the Flash X-ray facility.

This chapter presented the equipment and device and describes the circuit setup used to conduct the experiment. Additionally, an overview of energy transfer in the experiment is discussed. The following chapter analyzes the data collected in this chapter and tabulates the results.

IV. ANALYSIS OF RESULTS

This chapter presents analysis of the experiment results and provides discussion on how to interpret the data.

A. DISCUSSION

In order to correlate the output waveform of the diode from and the average dose of the TLDs, the charge (Q) collected in the diode was calculated using two different methods. The charge collected is proportional to the photocurrent (I_p) produce in the diode. The equation used for charge collected

$$Q = \frac{Vt}{R_L}, \tag{4.1}$$

where V is the voltage waveform, R_L is the scope termination resistance load and t is the time interval. The two methods were used to relate to absorbed dose. Data obtained from Figures 15– 20 were used for calculations in both methods. The first method used calculated the peak of the voltage waveform and the second method calculated the waveform integral in MATLAB. The area under the voltage waveforms of the figures were calculated using the integration function in MATLAB. Ten data points were used from the output plots to calculate the area under the waveform for the integral approach. For the first method, the collected charge is calculated using Equation (4.1) using the resistance load of 50 Ohms and time interval of 10 ns. An important factor that had to be determined was the mass of the active volume of the device. This was found by multiplying the density of silicon and the depletion depth at the reverse bias voltage of 25 VDC. Then the calculated dose could be determined by dividing the collected charge by the mass of the active volume. Tables 2 and 3 are the calculated dose of the output waveform plots from Figures 15–20 in comparison with TLD dose in units of roentgen. The calculated dose using the voltage amplitude peak showed average correlation to the TLD readings of +2%. The calculated dose using the voltage integral exhibited average correlation of +20% to the TLD measurements.

Dist (cm)	Voltage (peak)	Charge Collected (Q)	Calculated Dose (R)	TLD Dose (R)	Correlation to TLD
3	1.80	3.40E-09	116.87	127.00	−8%
6	1.50	1.50E-09	51.56	68.20	−25%
9	1.25	1.20E-09	41.25	42.10	−2%
12	0.98	9.85E-10	33.86	29.40	+12%
15	0.78	6.27E-10	21.56	20.50	+5%
18	0.67	6.73E-10	23.13	16.24	+30%
Average correlation to TLD					+2%

Table 2. Calculated dose using voltage waveform peak.

Dist(cm)	Waveform Area	Collected Charge (Q)	Calculated Dose (R)	TLD Dose (R)	Correlation to TLD
3	2.31E-07	4.61E-09	158.47	127.00	+20%
6	1.29E-07	2.57E-09	88.48	68.20	+23%
9	8.31E-08	1.66E-09	57.15	42.10	+26%
12	4.54E-08	9.08E-10	31.21	29.40	+6%
15	3.54E-08	7.09E-10	24.36	20.50	+16%
18	3.35E-08	6.69E-10	23.00	16.24	+30%
Average correlation to TLD					+20%

Table 3. Calculated dose of voltage waveform integral using MATLAB.

The calculated dose was converted to rad(Si) using the conversion factor for 1 roentgen of 1 MeV photons equals 1.95×10^{9} photons/cm^2. This fluence of 1 MeV photons is equivalent to 0.865 rad(Si) [Ref. 2]. The approximate dose rate can now be determined over the duration of the assumed pulse width of 10 ns. Both methods of voltage amplitude peak and voltage integral were calculated in Table 4.

	Voltage peak		Voltage integral	
Dist(cm)	Absorbed Dose rad(Si)	Dose Rate rad(Si)/s	Absorbed Dose rad(Si)	Dose Rate rad(Si)/s
3	101.01	1.01E+10	137.08	1.37E+10
6	44.60	4.46E+09	76.54	7.65E+09
9	35.68	3.57E+09	49.43	4.94E+09
12	29.29	2.93E+09	26.99	2.70E+09
15	18.65	1.86E+09	21.07	2.11E+09
18	20.01	2.00E+09	19.89	1.99E+09

Table 4. Dose rate approximations in rad(Si)

The first method looked at the initial energy being dissipated and provided a closer average correlation to TLD readings. The advantage of calculating dose using the first method was the ease of taking the voltage peak and multiplying it by the assumed pulse width. This allowed a quick analysis of the output pulse. The peak approach essentially

examines the initial "prompt" energy from the event. The voltage integral calculation took into account of all the mechanisms and energy losses taking place within the diode and the transmission line. A large amount of energy within the output pulse is being reflected back through the transmission line which accounts for a significant amount of error. Also, calculating the voltage integral was more time consuming and required more steps because the results had to be calculated with MATLAB.

Prior to starting the experiment, it was believed that the intensity would drop off as $1/R^2$ where R is the distance from the anode center axis faceplate. This is assumed according to the inverse square law where the intensity from a pointlike source would decrease as the inverse square of the distance. This data appears to show a dose-distance dependence between $1/R$ and $1/R^2$. Figure 22 compares the TLD dose readings with the calculated dose using the voltage peak and voltage integral. The figure shows that the calculated dose using the voltage peak has an overall closer correlation to the TLD readings than the calculated dose using the voltage integral. The dose readings at the shorter ranges illustrate the variation involving the two methods of calculation.

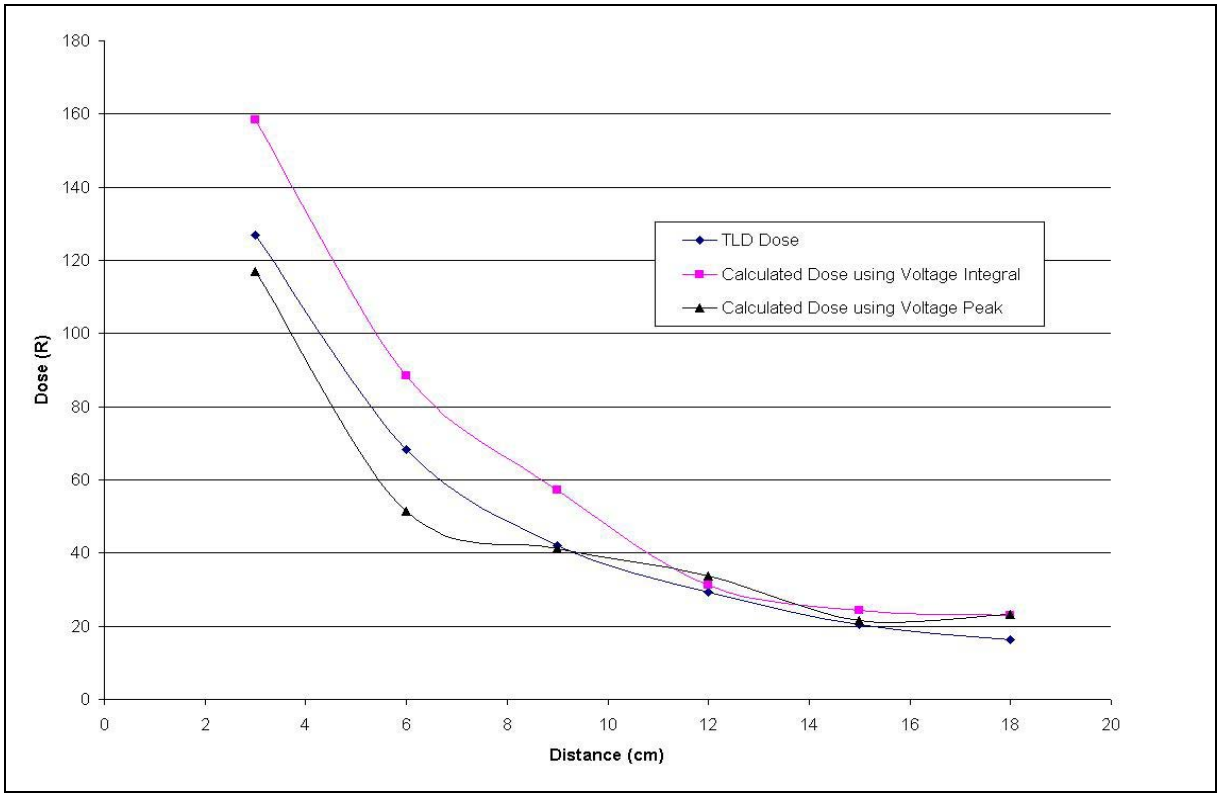

Figure 22. TLD and Calculated Doses vs. Distance.

B. LIMITATIONS OF THE RESULTS

Since dosimetry involves the indirect measurement of energy deposited, there will always be inherent limitations. First and foremost, the transfer of energy from one medium to another results in energy losses. The detection efficiency is limited by the small area of both the TLDs and PIN diode. These efficiencies dramatically decrease as the amount of energy increases even though the detector signal might increase. Furthermore, there are losses as the captured charge is converted to an electrical signal to be transmitted through coaxial cable to the oscilloscope. This is caused the characteristic impedance and reflection in the coaxial cable.

This chapter analyzed the data collected and tabulated the results of the experiment. These results were compared to the TLD readings to determine which method of calculating the diode output was more effective. Chapter V provides a summary of the conclusions reached from this experiment and recommendations for future use and studies.

V. SUMMARY

A. CONCLUSIONS

In practical dosimetry, precise measurement of dose is neither possible nor necessary. The key to dosimetry is the precision of the technique being used and being able to compare the result at any given time under the same conditions. Also knowledge of the radiation and its affect of semiconductor devices must be understood. This thesis analyzed the output radiation dose of the NPS Flash X-ray facility using silicon PIN diodes. The output waveform was used to calculate the collected charge and compare to the absorbed dose in CaF_2:Mn thermoluminescent dosimeters (TLDs). It has been concluded that the silicon detectors can provide a measurement able to be compared with TLD readings. In analyzing the output of the PIN diode waveform, it was determined that calculating the voltage waveform amplitude peak correlates more closely to the TLD readings than calculating waveform integral. Calculating the waveform amplitude peak does account for the majority of the energy transferred in the voltage waveform pulse. In integrating the waveform, a portion of the pulse is a result of the energy being dispersed by the transmission line which is independent of the pulse characteristics. A more precise measurement of the radiation output would require the analysis of the energy spectrum of the Flash X-ray facility.

B. RECOMMENDATION FOR FUTURE USE AND STUDIES

Dosimetry conducted at NPS linear accelerator facility (LINAC) uses scintillation of a phosphor captured by a secondary emissions monitor (SEM) as well as thermoluminescent dosimeters. Techniques used in this thesis can be applied at the NPS LINAC. Modification of the circuit and analysis of the captured signal would be required as the output radiation differs from the Flash X-ray facility. Also a detailed analysis of the diode would be required as degradation of the device would increase because the LINAC operates continuously over a greater period of time.

The following recommendations are suggested for to for continued studies in this area of research:

- Experimentation with several PIN diodes from different manufacturer to determine if similar results occur.
- Determination of energy spectrum of the Flash X-ray facility to confirm optimal semiconductor material for X-ray radiation detection.
- Determine frequency response and detection efficiency of the PIN diodes to optimize detection.
- Apply the similar techniques to the electron linear accelerator facility (LINAC) for radiation detection with appropriate circuit modification to analyze the desired radiation particle.
- Analyze diodes over a period to determine any significant degradation to would reduce the performance of the device.

APPENDIX A. SEMICOA SCA001C DATA SHEET

This Appendix is the data and specification sheets that describe the Semicoa SCA001C Silicon PIN diode.

SEMICOA

SCA001C 8041 Chip
Silicon PIN Photodiode

Data Sheet

Description

The SCA-001C is a high sensitive silicon PIN photodiode for use in low light applications across the spectral range of 320nm to 1100 nm.

This N-type photodiode offers high speed, low capacitance, and high breakdown voltage characteristics.

The standard version of model SCA-001C is housed in a hermetically sealed electrically isolated TO-18 or TO-46 metal case. It is also available in custom packages and in chip form for hybrid circuit boards.

This device is capable of meeting MIL-PRF-19500 requirements for environmental integrity and reliability.

Please contact Semicoa for special configurations
www.*SEMICOA*.com or (714) 242-3007

Applications

- Medical Analytical Instruments
- Optical Power Meters
- Densitometers
- Radiometers
- Optical Spectroscopy

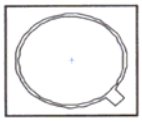

Features

- Photoconductive or Photovoltaic
- High-Reliability Hermetic Package
- Available in chip form and low profile TO-46 (-LP)
- Spectral Response from 320 to 1100nm

Benefits

- Low Dark Current
- Low Capacitance
- Fast Rise Time
- High Responsivity

Absolute Maximum Ratings

Parameter	Symbol	Rating	Unit
Operating Temperature	T_{OP}	-50 to +120	°C
Storage Temperature	T_{STG}	-55 to +150	°C
Soldering Temperature (t ≤ 5 seconds)	T_{SOL}	260	°C

SEMICOA SEMICONDUCTORS

Data Sheet No. SCA-001C

Type 001C

Generic Part Number:

001C

Geometry 8041

Request Quotation

Features:

- Photoconductive
- Low Dark Current
- Large Area

Applications:

- Medical Analytical Instruments
- Optical Power Meters
- Densitometers
- Radiometers

Semicoa's SCA-001C is a compact P-on-N type photodiode which offers the high speed, low capacitance, and high breakdown voltage associated with photoconductive diodes.

The standard version of model SCA-001C is housed in a compact, hermetically sealed, TO-18 metal case, which has a cap diameter of only 4.70 mm. The case is electrically isolated from the anode and cathode, thus allowing close spacing of components on a circuit board. This device is capable of meeting MIL-S-19500 requirements for environmental integrity and reliability. The SCA-001C is also available in custom packages and in a chip version for use on hybrid circuit boards. Please contact Semicoa for any special configurations.

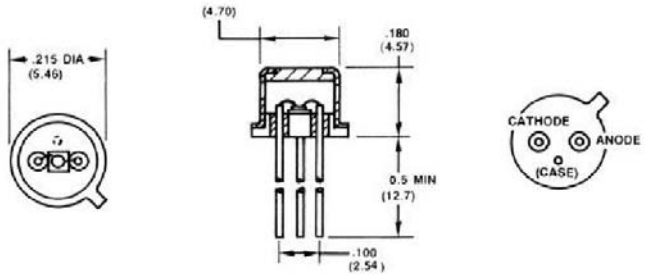

all curves at T_A = 25°C unless otherwise specified

CHARACTERISTIC CURVES

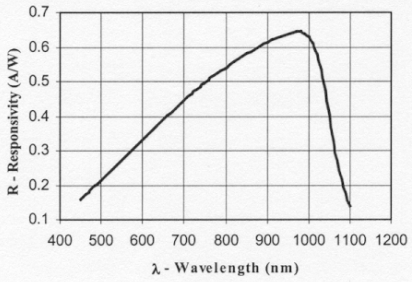

Figure 1 Responsivity vs Wavelength

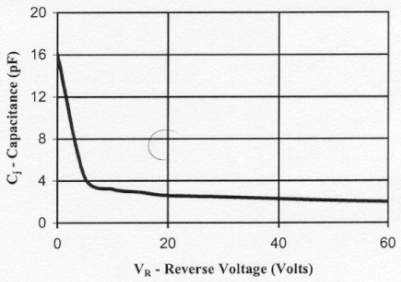

Figure 2 Capacitance vs Reverse Voltage

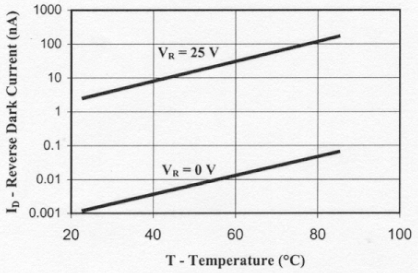

Figure 3. Reverse Current vs Temperature

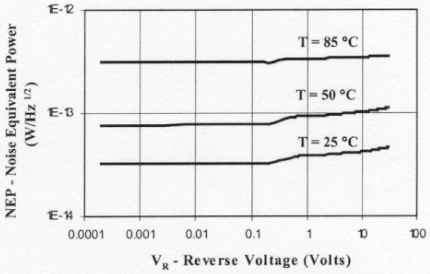

Figure 6 Noise Equivalent Power vs Reverse Voltage

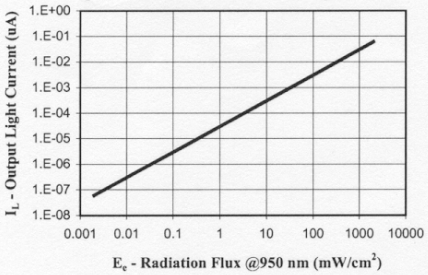

Figure 5. Light Current vs Irradiance @ λ = 950 nm

SEMICOA

SCA001C 8041 Chip

Silicon PIN Photodiode

Data Sheet

Description

The SCA-001C is a high sensitive silicon PIN photodiode for use in low light applications across the spectral range of 320nm to 1100 nm.

This N-type photodiode offers high speed, low capacitance, and high breakdown voltage characteristics.

The standard version of model SCA-001C is housed in a hermetically sealed electrically isolated TO-18 or TO-46 metal case. It is also available in custom packages and in chip form for hybrid circuit boards.

This device is capable of meeting MIL-PRF-19500 requirements for environmental integrity and reliability.

Please contact Semicoa for special configurations
www.*SEMICOA*.com or (714) 242-3007

Applications

- Medical Analytical Instruments
- Optical Power Meters
- Densitometers
- Radiometers
- Optical Spectroscopy

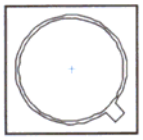

Features

- Photoconductive or Photovoltaic
- High-Reliability Hermetic Package
- Available in chip form and low profile TO-46 (-LP)
- Spectral Response from 320 to 1100nm

Benefits

- Low Dark Current
- Low Capacitance
- Fast Rise Time
- High Responsivity

Absolute Maximum Ratings

Parameter	Symbol	Rating	Unit
Operating Temperature	T_{OP}	-50 to +120	°C
Storage Temperature	T_{STG}	-55 to +150	°C
Soldering Temperature (t ≤ 5 seconds)	T_{SOL}	260	°C

SEMICOA

SCA001C 8041 Chip

Silicon PIN Photodiode

Data Sheet

DEVICE CHARACTERISTICS

characteristics specified at T_A = 25°C

Mechanical Characteristics			
Active Diameter	d	0.04	Inches
Active Area	A	0.81	mm^2

Optical Characteristics			
Spectral Response	λ	320 to 1100	nm
Peak Sensitivity Wavelength	λ_p	950	nm

Electrical Characteristics

Parameter	Symbol	Test Conditions	Min	Typ	Max	Units
Dark Current	I_D	V_R = 1 mV V_R = 25 V		0.01 0.10	1.0 10	pA nA
Responsivity	R	λ = 900 nm λ = 632 nm λ = 560 nm	0.50 0.35 0.25	0.67 0.43 0.33		A/W
Risetime	t_r	V_R = 25 V, R_L = 50 Ω		5		nS
Capacitance	C_j	V_R = 25 V, f = 1 MHz		2.0	5.0	pF
Reverse Breakdown Voltage	BV_R	I_R = 10 μA	100	200		V
Forward Voltage	V_F	I_F = 1 mA		0.6	1.0	V
Shunt Resistance	R_{sh}	V_R = 1 mV	1.0	6.0		GΩ
Series Resistance	R_S			10	20	Ω
Noise Equivalent Power	NEP			$5x10^{-15}$		W/√Hz

Package Specifications — typical dimensions shown

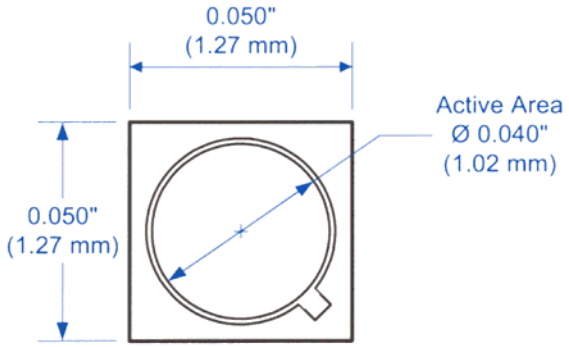

The junction depth of the SCA-001C is in the range of 0.7 to 1.0 um.

The chart below shows the depletion width versus reverse bias voltage.

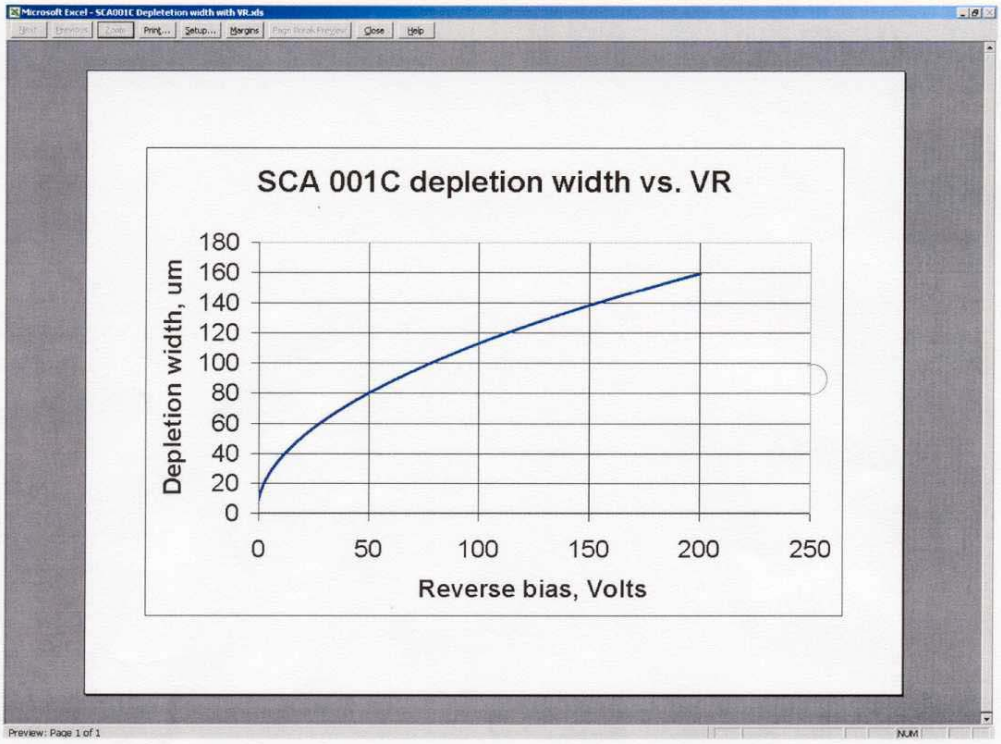

LIST OF REFERENCES

1. G. F. Knoll, *Radiation Detection and Measurement*, 3rd Edition, John Wiley, New York, 2000.

2. A. Holmes-Siedle and L. Adams, *Handbook of Radiation Effects*, 2nd Edition, Oxford, New York, 2002.

3. F. H. Attix and W. C. Roesch, *Radiation Dosimetry Vol. 1: Fundamentals*, 2nd Ed., Academic Press, New York, 1968.

4. A. C. Thompson and D. Vaughan, "X-ray Data Booklet" [http://xdb.lbl.gov/], U.S. Department of Energy, January 2001.

5. "ASTM Standard E 668-93 Standard Practice for Application of Thermoluminescent-Dosimetry (TLD) Systems for Determining Absorbed Dose in Radiation-Hardness Testing of Electronic Devices," Copyright ASTM, West Conshohocken, Pennsylvania, 1996.

6. R. F. Pierret, *Semiconductor Device Fundamentals*, Addison-Wesley, Reading, Massachusetts, 1996.

7. G. Bertolini, and A. Coche, *Semiconductor Detectors*, American Elsevier, New York, 1968.

8. R. B Pietruszka, "Operation and Characteristics of the Flash X-ray Generator at the Naval Postgraduate School," Master's Thesis, Naval Postgraduate School, Monterey, California, 1989.

9. Semicoa Semiconductors, Inc. "Semicoa Data Sheet: SCA001C" [http://www.semicoa.com], January 2003.

10. Vicotoreen, Inc. *Instruction Manual for Model 2800 Thermoluminescence Dosimeter Reader*, Cleveland, Ohio, September 1986.

11. N. J. Rudie, *Principles and Techniques of Radiation Hardening Vol. 1*, 3rd Edition, Western Periodicals, North Hollywood, California, 1986.

12. S. Deme, *Semiconductor Detectors for Nuclear Radiation Measurement*, Wiley-Interscience, New York, 1971.

13. R. Eisberg and R Resnick, *Quantum Physics of Atoms, Molecules, Solids, Nuclei and Particles*, John Wiley, New York, 1974.

THIS PAGE INTENTIONALLY LEFT BLANK

INITIAL DISTRIBUTION LIST

1. Defense Technical Information Center
   Ft. Belvoir, Virginia

2. Dudley Knox Library
   Naval Postgraduate School
   Monterey, California

3. Professor John P. Powers
   Naval Postgraduate School
   Monterey, California

4. Professor Todd R. Weatherford
   Naval Postgraduate School
   Monterey, California

5. Mr. Andrew A. Parker
   Naval Postgraduate School
   Monterey, California

6. Mr. Donald D. Synder
   Naval Postgraduate School
   Monterey, California